Utilization of Spatio-temporal image for LED array acquisition in Road to Vehicle Visible Light Communication

Syunsuke Usui
Graduate student, Nagoya University
Nagoya University, Furo-cho, Chikusa-ku, Nagoya, 464-8603, JAPAN
TEL: +81-52-789-2729, FAX: +81-52-789-3173,
E-mail: usui@katayama.nuee.nagoya-u.ac.jp
Takaya Yamazato
Professor, Nagoya University
Furo-cho, Chikusa-ku, Nagoya, 464-8603, JAPAN
E-mail: yamazato@ nuee.nagoya-u.ac.jp
Shintaro Arai
Research associate, Kagawa National College of Technology
551 Kohda, Takuma-cho, Mitoyo, Kagawa, 769-1192, JAPAN
E-mail: arai@cn.kagawa-nct.ac.jp
Tomohiro Yendo
Associate professor, Nagaoka University of Technology
1603-1 Kamitomioka, Nagaoka, Niigata, 940-2188, JAPAN
E-mail: yendo@nagaokaut.ac.jp
Toshiaki Fujii
Professor, Nagoya University
Furo-cho, Chikusa-ku, Nagoya, 464-8603, JAPAN
E-mail: fujii@ nuee.nagoya-u.ac.jp
Hiraku Okada
Associate professor, Nagoya University
Furo-cho, Chikusa-ku, Nagoya, 464-8603, JAPAN
E-mail: okada@ nuee.nagoya-u.ac.jp

ABSTRACT

In this paper, we focus on visible light communication systems for road-to-vehicle communications (R2V-VLC). We use an LED array as a transmitter and a high-speed camera as a receiver. To implement R2V-VLC, it is necessary for the receiver to search the target LED array from the captured images (LED array acquisition) before data demodulation. We propose a new approach for LED array acquisition. We present a new perspective on the channel whereby the channel can be represented by a three-dimensional spatio-temporal image. We show LED array in the spatio-temporal image has high time-gradient value and low space-gradient value. Using such characteristic gradient values, we propose a new LED array acquisition method. As the results of the experiment in driving situation, we can achieve acquisition miss rate = 0%.

Keywords: LED, ITS, Road-to-Vehicle Communication, Visible Light Communication, Spatio-temporal image, LED array acquisition

1. INTRODUCTION

Light-emitting diodes (LEDs) offer a new and revolutionary light source that save energy. LEDs emerge as a popular green light. Since LEDs are solid-state lighting devices, LEDs can be modulated at high speeds that are undetectable to the human eye. Thus, it is possible to transmit data with LED devices while it is illuminating and/or displaying image. Because of this advantage, Visible light communications (VLC) using LED have attracted a great deal of attention as novel communication systems [1] - [4].

There are many LED lights in road traffic, traffic light, signage board, street and area lights, automotive headlights, and brake lights. These LEDs attract VLC applications in the field of intelligent transport systems (ITS) [3], [4]. For examples, LED traffic lights broadcast driving assistances information to cars or LED brake lights transmit warning information to a behind car and so on. Among VLC for ITS, this paper focuses on a road-to-vehicle visible light communication (R2V-VLC) using an LED array, assumed to be a transmitter, and an in-vehicle high-speed camera as a receiver. As advantages of this R2V-VLC, this communication does not suffer from multipath as classical radio communication due to the directional characteristic of LED light. We also note that the installation of transmitters is much easier because LED traffic lights or LED signage boards that have already been installed can be used. A parallel data transmissions are possible by modulating each LED luminance individually if we use a high-speed camera as a receiver.

In R2V-VLC, a blinking pattern of LEDs represents data. The data demodulation is performed by extracting luminance corresponding to each of LEDs from images captured by high-speed camera. Hence, it is necessary for the receiver to search the target LED array from the captured images. This process, LED array acquisition, must be completed before data demodulation. If LED acquisition is failed, data demodulation cannot be implemented. Therefore, LED array acquisition has a significant role for R2V-VLC. LED array acquisition requires to prevent following two issues; true-negative (missing of the target LED array), and false-positive (any things other than the target LED array is acquired).

In [5], frame difference acquisition method is proposed. This method subtracts two successive images. As the high-speed camera captures every image in high frame rate, most of the background image other than LED array can be eliminated. In this way, the acquisition is achieved. However, the background image cannot be eliminated completely because of vibrations associated with vehicle movement. As a result, false-positive still occurs. To reduce the effect of such vibrations, Shiraki et al. apply the block matching method to LED array acquisition [6]. This method calculates corresponding position between two successive images and corrects positional relationship between them. Using such relationship, this method reduces false positive. However, this method tends to mistake corresponding position calculation at LED array, and it leads true-negative in case of data transmission.

In this paper, we propose a new approach for LED array acquisition. We focus on a spatio-temporal image and a spatio-temporal cross-section image. Spatio-temporal image is three-dimensional space image made by arranging captured images in time series. Since blinking LED changes its own luminance value rapidly, LEDs in LED array have high partial differential value (gradient value) in time-domain of spatio-temporal image. Since each of LEDs changes its status simultaneously from on to off or off to on, LEDs in LED array have low partial differential value (gradient value) in space-domain of spatio-temporal image. Using both characteristic values in time-domain and space-domain, we propose a new LED array acquisition method that can prevent both true-negative and false-positive. As the results of the experiment in driving situation, we achieve that true-negative does not occur although the vehicle is vibrating.

This paper is organized as follows; Section 2 presents R2V-VLC system used in this paper. Section 3 introduces spatio-temporal image and spatio-temporal cross-section image and presents partial differential of luminance value of spatio-temporal image in time domain and space domain. Section 4 presents LED array acquisition method. Section 5 shows experimental result. Finally, conclusions are presented in Sec. 6.

2. SYSTEM OVERVIEW

Figure 1 shows a block diagram of system used in this paper. A transmitter consists of 256 LEDs arranged in 16×16 square matrix and a modulator. The transmitter applies On-Off Keying (OOK) and each of LED is modulated by the OOK signal.

A receiver consists of a high-speed camera, an image processing unit and a decoder. The transmitted LED array blinking passes through the optical channel and is captured by the high-speed camera. The image processing unit determines the position of each LED and extracts the LED luminance. The image processing unit consists of four units necessary for the data detection in a driving situation; LED array acquisition, LED array tracking, LED position estimation and luminance normalization. This paper focuses attention on LED acquisition. The others are described in [7] . In LED acquisition unit, the receiver searches the LED array from the captured images. As a result of image processing, the receiver extracts luminance corresponding to each of LED from captured images. Using this luminance value and its position, the receiver demodulates and outputs received data.

The LED array acquisition process is the first image processing to search the target LED array from a captured whole image. Figure 2 shows an example of captured images in time series. The high-speed camera outputs at intervals of frame rate. When a LED is on, the LED in captured image has high luminance value. When a LED is off, it has low luminance value.

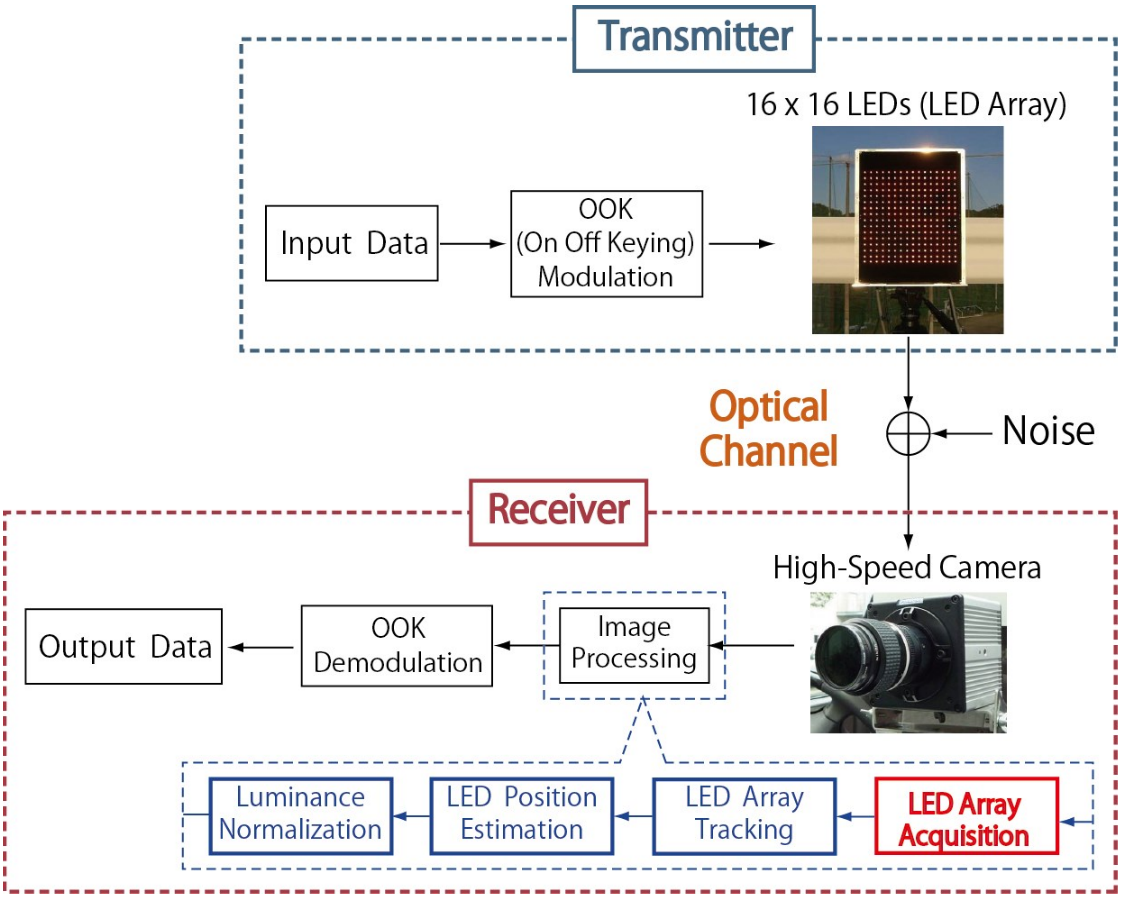

Figure 1. System model.

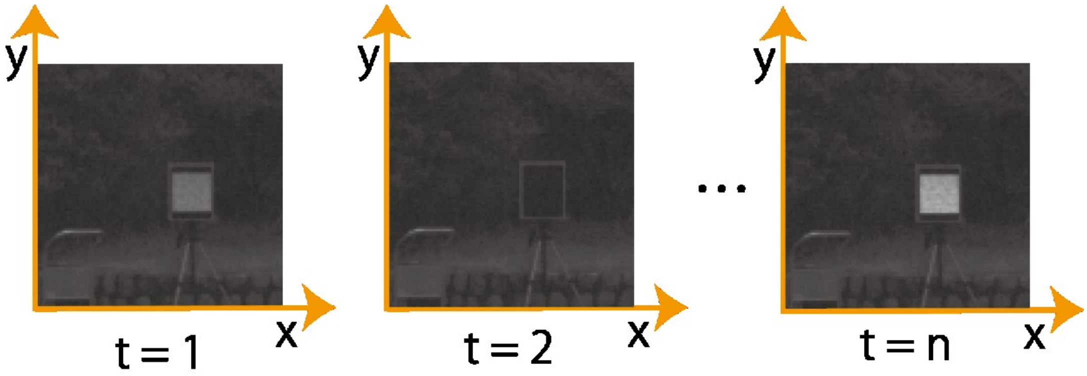

Figure 2. Example of captured images in time series.

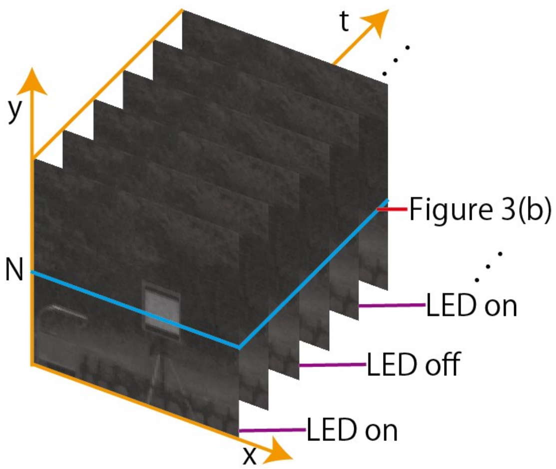

(a) Spatio-temporal image.

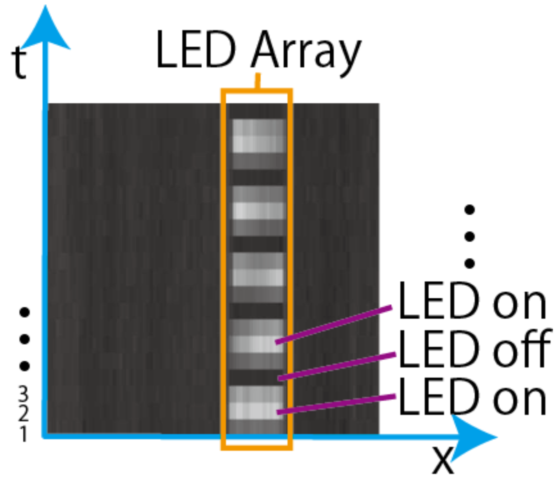

(b) Spatio-temporal cross-section image.

Figure 3. Spatio-temporal image and spatio-temporal cross-section image.

3. LED ARRAY IN SPATIO-TEMPORAL IMAGE

3.1 Spatio-temporal image

Now let us arrange the captured images of Fig.2 as shown in Fig.3 (a). This three-dimensional discrete space is called Spatio-temporal image. From the 3D spatio-temporal image, let us create a 2D plane of (x, t) at y=N as shown in Fig.3 (b). This cross-section image is called Spatio-temporal cross-section image.

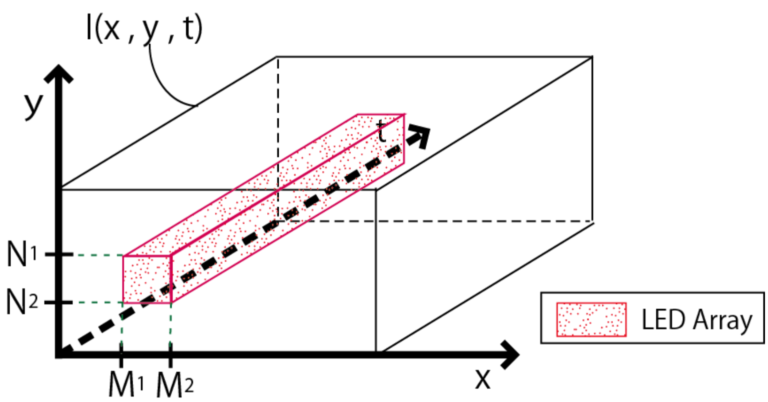

Figure 4. Spatio-temporal image model with LED array.

As LED array is a constellation of single LEDs. Let us assume LED array and high-speed camera remain still and each of LED changes its status simultaneously from on to off, or off to on. Figure 4 shows the spatio-temporal image for LED array. Let us define this spatio-temporal image has luminance value $I\,(x, y, t)$, and assume that the LED array stays in the region $D\{x \mid M_1 \leqq x \leqq M_2,\ y \mid N_1 \leqq y \leqq N_2\}$.

3.2 Partial differential of luminance value of spatio-temporal image in time domain

Now let us focus attention on blinking of LED in time-domain. As described in Sec.2, when an LED is on, LED in captured image has high luminance value. When an LED is off, it has low luminance value. Therefore, luminance values of LED may change considerably in time-domain. We recognize that also from Fig.3 (b). In other words, LED array has high time-gradient value.

Let us define $\frac{\delta}{\delta t} I(x, y, t)$ as a partial differentiation of luminance value $I\,(x, y, t)$ in time-domain.

Then, $\frac{\delta}{\delta t} I(M, N, t)\ \{M, N \in D\}$ takes a large value.

3.3 Partial differential of luminance value of spatio-temporal image in space domain

Now let us focus attention on blinking of LED in space-domain. As assumed in Sec.3.1, each LED has nearly same luminance value as shown in Fig.3 (b). In other words, LED array has low space-gradient value.

Let us define $\frac{\delta}{\delta x}\frac{\delta}{\delta y} I(x, y, t)$ as a partial differentiation of luminance value $I\,(x, y, t)$ in space domain. Then, $\frac{\delta}{\delta x}\frac{\delta}{\delta y} I(M, N, t)\ \{M, N \in D\}$ takes a small value.

3.4 Effect of LED diffusion

If a LED is near by other LEDs, a ray of LED interferes with other ray of LED due to the diffusion of LEDs [8] . Figure 5 shows this interference. Because of interference, the focused LED affects not only the actual corresponding pixel but also its surrounding pixels. Then, the luminance distribution of LED array becomes flat at captured image. As a result, time-gradient may not be a high value and space-gradient may not be a low value. Hence, we should take into account both gradient values in time-domain and it in space-domain.

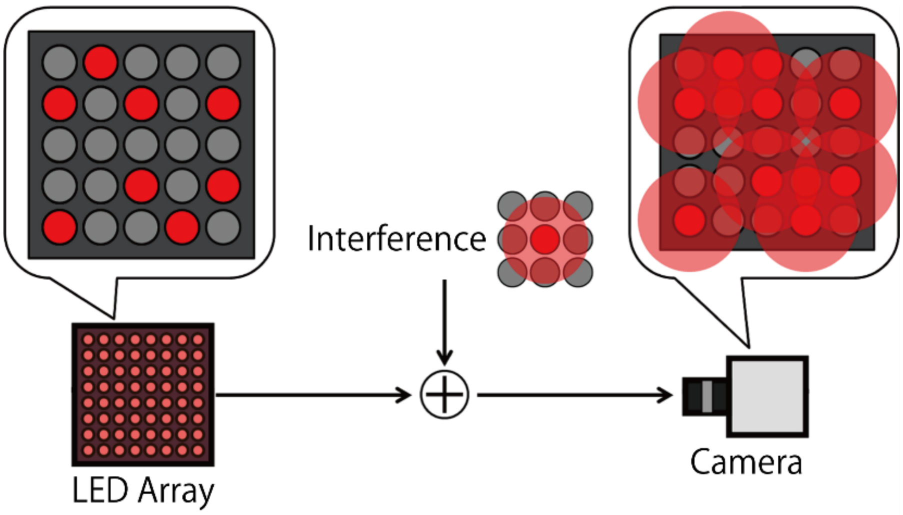

Figure 5. Image of interference.

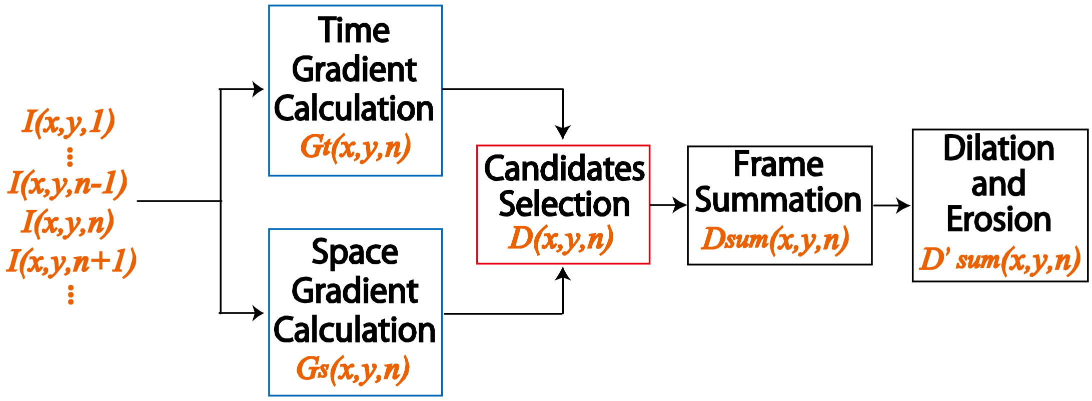

Figure 6. Block diagram of proposed LED array acquisition method.

4. LED ARRAY ACQUISITION METHOD

This section explains proposed LED array acquisition method. Figure 6 shows a block diagram of LED array acquisition method. This method calculates the time-gradient value and space-gradient value, then this method regards the pixel that have high time-gradient value and low space-gradient value as LED array.

4.1 Time / Space gradient calculation

In the LED array acquisition method, we first calculate the time-gradient and space-gradient. From the discussion of Sec.3, LED array has high time-gradient value and low space-gradient value. We calculate them by filtering the input image I (x, y, t). We use Sobel operator for filtering. It is used for edge detection in image processing [9] .

In case of t=n, time gradient value G_t (x, y, n) and space gradient value G_s (x, y, n) are calculated by the following equations, respectively

$$G_t(x,y,n) = \sqrt{\{\sum_{k=-1}^{1}\sum_{l=-1}^{1} s_1(k,l)\cdot I(x+k,y,n+l)\}^2 + \{\sum_{k=-1}^{1}\sum_{l=-1}^{1} s_1(k,l)\cdot I(x,y+k,n+l)\}^2} \qquad (1)$$

$$G_s(x,y,n) = \sqrt{\{\sum_{k=-1}^{1}\sum_{l=-1}^{1} s_1(k,l)\cdot I(x+k,y+l,n)\}^2 + \{\sum_{k=-1}^{1}\sum_{l=-1}^{1} s_2(k,l)\cdot I(x+k,y+l,n)\}^2} \qquad (2)$$

where s_1 (k, l) and s_2 (k, l) are filtering kernels of Sobel operator. They are represented by the following.

$$s_1(k,l) = \begin{pmatrix} -1 & -2 & -1 \\ 0 & 0 & 0 \\ 1 & 2 & 1 \end{pmatrix} \quad , \quad s_2(k,l) = \begin{pmatrix} -1 & 0 & 1 \\ -2 & 0 & 2 \\ -1 & 0 & 1 \end{pmatrix} \qquad (3)$$

4.2 LED array candidates selection

Next step is a candidate selection process. LED array has high G_t (x, y, n) and low G_s (x, y, n). Hence, the LED array candidates image $D(x, y, n)$ is selected by the following.

$$D(x,y,n) = \begin{cases} 255 & G_t(x,y,n) > \varphi_t \cap G_s(x,y,n) < \varphi_s \\ 0 & otherwith \end{cases} \qquad (4)$$

Here φ_t denotes the threshold value in time-domain and φ_s denotes the threshold value in space-domain. As shown in Eq. (4), $D(x, y, n)$ is a binary image.

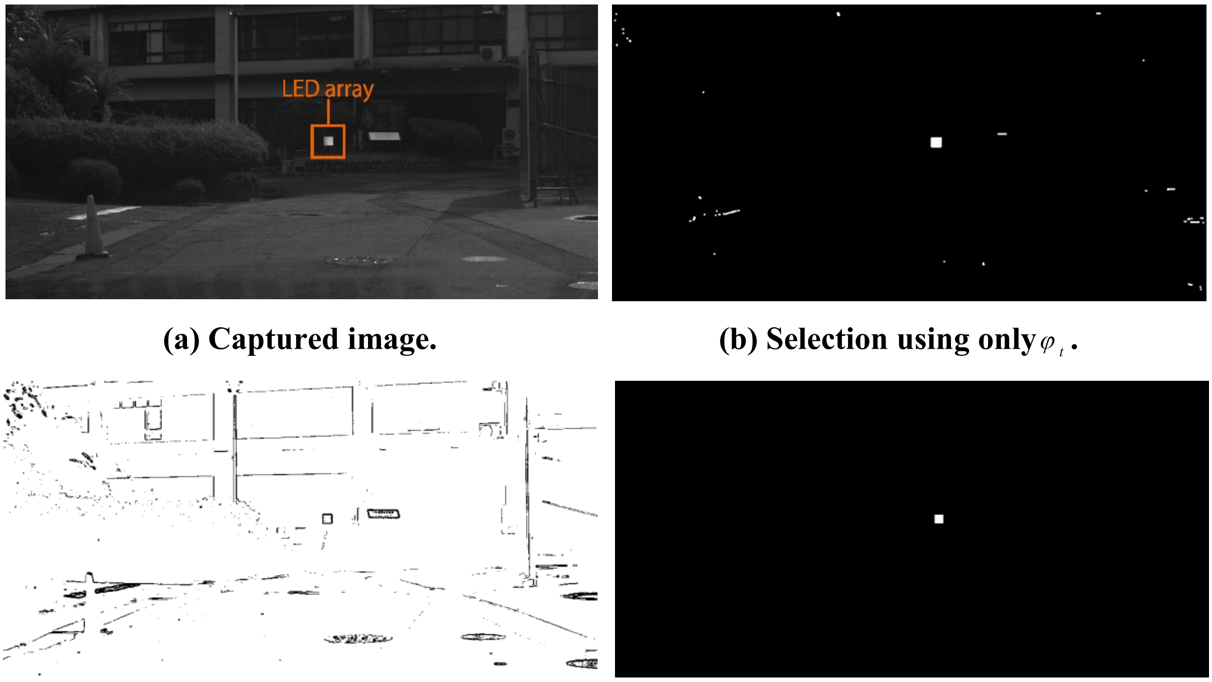

(a) Captured image. **(b) Selection using only φ_t.**

(c) Selection using only φ_s. **(d) Selection using both φ_t and φ_s.**

Figure 7. Selection results.

The advantage of using both φ_t and φ_s is following; Figure 7 (a) shows a captured image with the target LED array. Figure 7 (b) shows a result of the selection using only φ_t. Further, Fig.7 (c) shows a result of the selection using only φ_s. As we see clearly from Fig.7 (b) and Fig.7 (c), selection using only φ_t or φ_s occurs false-positive. On the other hand, as shown in Fig.7 (d), selection with both φ_t and φ_s does not occur false-positive. Using both φ_t and φ_s, we can prevent false-positive. However, it may sometimes happen true-negative.

4.3 Frame summation・Dilation and erosion

Gradient calculation and LED array candidates selection at each frame is executed independently. Even when LED array is not selected in $D(x, y, n)$, there is a possibility that LED array is selected in $D(x, y, n\text{-}1)$. Hence, to select LED array more correctly, we sum $D(x, y, t)$ from $t=n$ to $t=n\text{-}k$ and generate an image $D_{sum}(x, y, n)$. $D_{sum}(x, y, n)$ is generated by the following.

$$D_{sum}(x, y, n) = D(x, y, n) \vee D(x, y, n-1) \vee \cdots \vee D(x, y, n-k) \tag{5}$$

where $\vee$ is OR operator (logical disjunction). In this paper, we employ $k = 4$. After frame summation process, this method performs dilation and erosion, that defuse petty noise, to $D_{sum}(x, y, n)$, and generates an image $D'_{sum}(x, y, n)$. We finally assume that the region that has luminance value 255 in $D'_{sum}(x, y, n)$ is the target LED array.

5. EXPERIMENTAL RESULT

5.1 Experimental setup

We performed experiments in driving situation as vehicle moves at 30 km/h. Figure 8 shows captured images with different distance, 30 m and 90 m. LED array in captured image is 21×21 pixel in the distance 30 m and is 7×7 pixel in the distance 30 m. Table 1 summarizes the parameters of the experiment.

(a) 30 m. **(b) 90 m.**

Figure 8. Captured images with different distance.

Table 1. Parameters of experiment.

Blinking frequency	500 Hz	Blinking pattern	*On/Off* , *Random*
Capturing frame rate	1000 fps	Vehicle speed	30 km/h
Distance from LED	30 m , 90 m	Weather / Time	Sunny / Daytime
Number of frames	200 frames	Image resolution	1024×512 pixel

(a) *On / Off*. **(b) *Random*.** **(c) Example of success.**

Figure 9. Blinking pattern and example of success.

We evaluate results of experiments by miss-rate versus the thresholds, φ_t and φ_s . Miss rate P_m is defined following the Eq. (6)

$$P_m = 1 - \frac{F_{correct}}{F_{all}} \tag{6}$$

Where F_{all} is the number of all frames, and $F_{correct}$ is the number of acquisition success frames. Acquisition success is defined by the following. We first make a circumscribing rectangle. That contains the region where luminance value 255 in $D'_{sum}(x, y, n)$. An example is shown in Fig.9 (c). We set the rectangle has +3 pixels larger than the true LED array. If the circumscribing rectangle contains all of the true LED array, we say acquisition succeeds.

We perform two cases of LED blinking patterns; *On/Off* and *Random* as shown in Fig.9 (a) and (b), respectively. *On/Off* represents the pattern that repeats all of the LEDs are on and off. *Random* is a case of data transmission so that each of LED blinks randomly. Note that we also include the inverted signal for LED array tracking used in [10].

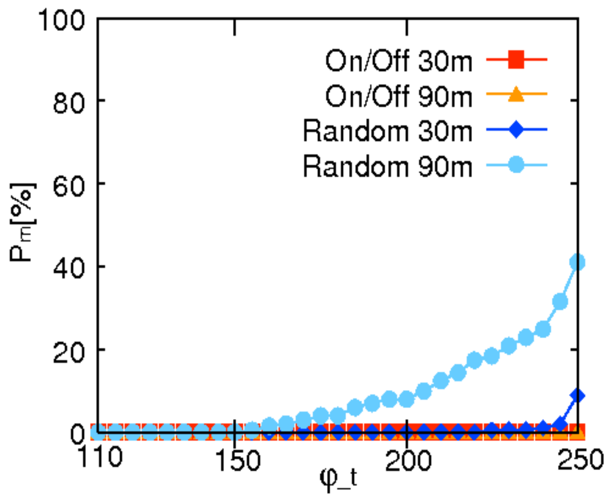

(a) P_m **versus** φ_t (φ_s = 80).

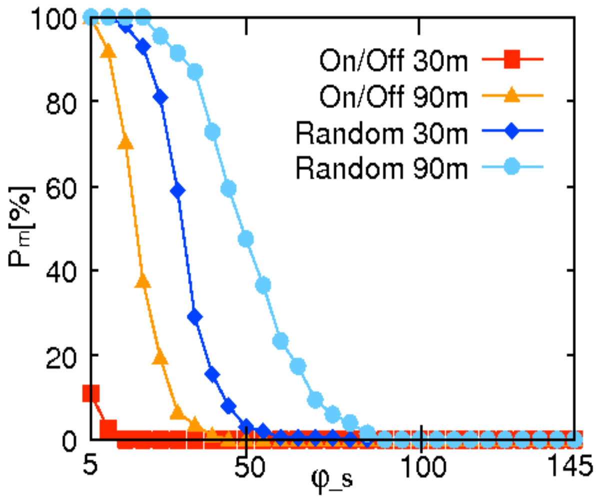

(b) P_m **versus** φ_s (φ_t = 180).

Figure 10. Experimental results.

As described in Sec.4, acquisition with only φ_t or φ_s occurs many false-positive. Hence we do not evaluate P_m for acquisition with only φ_t or φ_s. On the other hand, in case of acquisition with both φ_t and φ_s, P_m changes depending on φ_t and φ_s.We evaluate P_m for each distance and blinking pattern varying φ_t and φ_s, respectively. We fix φ_s = 80 when we evaluate the effect of φ_t, and fix φ_t = 180 when we evaluate the effect of φ_s. φ_t and φ_s are within $110 \leqq \varphi_t \leqq 250$, $5 \leqq \varphi_s \leqq 145$, respectively. We vary them every five values.

5.2 Experimental Results

Figure 10 (a) shows P_m versus φ_t. In case of *On/Off*, P_m becomes 0% all φ_t because LED array with *On/Off* has extremely high time-gradient value. On the other hand, in case of *Random*, P_m becomes 0% when φ_t is less than 220 in the distance 30 m, and P_m becomes 0% when φ_t is less than 150 in the distance 90 m. It is because LED array with *Random* has lower time-gradient value than with *On/Off* due to interference between LEDs. This interference decreases high-frequency component of captured images. As a result, time-gradient value of LED array with *Random* decreases. Further, in case of 30 m, P_m is lower than in case of 90 m. This reason is given as follows. The farther high speed camera from LED array, the smaller LED array in captured image is. Then LED array acquisition becomes more difficult. Although LED array in captured image is small (7×7 pixel) in the distance 90 m, we can achieve P_m = 0% by setting an appropriate φ_t. We confirm LED array has high time-gradient value.

Figure 10 (b) shows P_m versus φ_s. In case of *On/Off*, P_m becomes 0% when φ_s is more than 15 in the distance 30 m, and P_m becomes 0% when φ_s is more than 45 in the distance 90 m. It is because LED array with *On/Off* has low time-gradient value. On the other hand, in case of *Random*, P_m becomes 0% when φ_s is more than 70 in the distance 30 m, and P_m becomes 0% when φ_s is more than 90 in the distance 90 m. LED array with *On/Off* has lower space-gradient value than that with *Random* since each of LED in case of *On/Off* have nearly same luminance value. Further, in case of 30 m, P_m is lower than in case of 90m.This reason is same in case of P_m versus φ_t. Although LED array in captured image is small (7×7 pixel) in the distance 90 m, we can achieve P_m = 0% by setting an appropriate φ_s. We confirm LED array has low space-gradient value.

6. CONCLUSIONS

In this paper, we have introduced the spatio-temporal image and spatio-temporal cross-section image to acquire LED array for R2V-VLC and have shown LED array in the spatio-temporal image has high time-gradient value and low space-gradient value. We have proposed new LED array acquisition that use both gradient values. As the results of the experiment in driving situation, we can achieve P_m = 0% by setting an appropriate, and although in the vehicle is vibrating.

7. ACKNOWLEDGEMENT

This work is supported in part by KAKENHI (23560449). We would like to note that discussions with Prof. Masaaki Katayama and Dr. Kentaro Kobayashi have been illuminating this research.

8. REFERENCES

[1] T. Komine, J. H. Lee, S.haruyama, and M. Nakagawa, "Adaptive equalization system for visible light wireless communication utilizing multiple white LED lighting equipment, " IEEE Transactions on Wireless Communications, vol. 8, no. 6, pp. 2892-2900, Jun. 2009.

[2] G.-K.-H.Pang, C.-H.Chan, and T.T.O.Kwan, "Tricolor Light-Emitting Diode Dot Matrix Display System with Audio Output", IEEE Transaction on Industry Application, vol.37, No.2, pp.534-540, Mar/Apr.2001

[3] M. Akanegawa, Y. Tanaka, and M. Nakagawa, "Basic study on traffic information system using LED traffic lights", IEEE Trans. on Intelligent Transportation Systems, vol. 2, no. 4, pp. 197-203, Dec. 2001.

[4] H. S. Liu and G. Pang, "Positioning beacon system using digital camera and LEDs", IEEE Trans. on Vehicular Technology, vol. 52, no. 2, pp. 406-419, Mar. 2003.

[5] M. Wada, T. Yendo, T. Fujii, M. Tanimoto, "Road-to-vehicle communication using LED traffic light", Intelligent Vehicles Symposium 2009 IEEE, pp. 179-184 , June 2009

[6] Y. Shiraki, T. Yamazato, H. Okada, T. Fujii, T. Yendo, S. Arai, "Multiple Information Sources Recognition Method for Ubiquitous Visible Light Communication Using on-Vehicle High-Speed Camera", The Transactions of the Institute of Electronics, Information and Communication Engineers, vol.J95-B, no.11, pp.1517-1528, Nov. 2011

[7] Y. Shiraki, T. Nagura, T. Yamazato, S. Arai, T. Yendo, T. Fujii, H. Okada, "Robust Receiver Design for Road-to-Vehicle Communication System Using LED Array and High-Speed Camera", 18th World Congress on Intelligent Transport Systems, Oct. 2011

[8] T. Kasashima ,T. Yamazato, H. Okada, T. Fujii, T. Yendo, S. Arai, "Cancellation Method for Intersymbol Interference on Road-to-Vehicle Visible Light Communication using LED Array and High-Speed Camera", Technical Report of IEICE, ITS2011-38, pp. 129-134, Feb. 2012

[9] William K. Pratt, *Digital Image Processing*, New York: a Wiley-Interscience publication, 1978.

[10] T. Nagura, T. Yamazato, M. Katayama, T. Yendo, T. Fujii, H. Okada, "Tracking an LED Array Transmitter for Visible Light Communications in the Driving Situation", IEEE International Symposium on Wireless Communication Systems (ISWCS2010), pp.765-769 Sept. 2010.